European Journal of Pharmaceutical Sciences 67 (2015) 144–159

Contents lists available at ScienceDirect

European Journal of Pharmaceutical Sciences

journal homepage: www.elsevier.com/locate/ejps

Modeling and design of challenge tests: Inflammatory and metabolic biomarker study examples

Johan Gabrielsson [a,*], Stephan Hjorth [h,1], Barbara Vogg [b], Stephanie Harlfinger [c], Pablo Morentin Gutierrez [d], Lambertus Peletier [e], Rikard Pehrson [f], Pia Davidsson [g]

[a] Department of Biomedical Sciences and Veterinary Public Health, Division of Pharmacology and Toxicology, Swedish University of Agricultural Sciences, Box 7028, SE-750 07 Uppsala, Sweden
[b] Novartis Institutes for Biomedical Research, DMPK/Nonclinical PK/PD, Fabrikstrasse 28, CH-4056 Basel, Switzerland
[c] Novartis Institutes for BioMedical Research, Metabolism and Pharmacokinetics, CH-4002 Basel, Switzerland
[d] AstraZeneca R&D Alderley Park, Oncology iMED, DMPK, 35F173, Macclesfield SK10 4TG, UK
[e] Mathematical Institute, Leiden University, PB 9512, 2300 RA Leiden, The Netherlands
[f] RIRA iMed DMPK, AstraZeneca R&D Mölndal, R&D, Innovative Medicines, S-431 83 Mölndal, Sweden
[g] CVMD iMed Translational Science, AstraZeneca R&D Mölndal, R&D, Innovative Medicines, S-431 83 Mölndal, Sweden
[h] CVMD iMed Bioscience, AstraZeneca R&D Mölndal, R&D, Innovative Medicines, S-431 83 Mölndal, Sweden

ARTICLE INFO

Article history:
Received 18 August 2014
Accepted 13 November 2014
Available online 28 November 2014

Keywords:
Mixture dynamics
Turnover models
Inhibitory drug action
Oral glucose tolerance test
Hormetic concentration–response relationship
Quantitative pharmacology

ABSTRACT

Given the complexity of pharmacological challenge experiments, it is perhaps not surprising that design and analysis, and in turn interpretation and communication of results from a quantitative point of view, is often suboptimal. Here we report an inventory of common designs sampled from anti-inflammatory, respiratory and metabolic disease drug discovery studies, all of which are based on animal models of disease involving pharmacological and/or patho/physiological interaction challenges. The corresponding data are modeled and analyzed quantitatively, the merits of the respective approach discussed and inferences made with respect to future design improvements. Although our analysis is limited to these disease model examples, the challenge approach is generally applicable to the vast majority of pharmacological intervention studies.

In the present five Case Studies results from pharmacodynamic effect models from different therapeutic areas were explored and analyzed according to five typical designs. Plasma exposures of test compounds were assayed by either liquid chromatography/mass spectrometry or ligand binding assays. To describe how drug intervention can regulate diverse processes, turnover models of test compound–challenger interaction, transduction processes, and biophase time courses were applied for biomarker response in eosinophil count, IL_6 response, paw-swelling, TNF_α response and glucose turnover *in vivo*. Case Study 1 shows results from intratracheal administration of Sephadex, which is a glucocorticoid-sensitive model of airway inflammation in rats. Eosinophils in bronchoalveolar fluid were obtained at different time points via destructive sampling and then regressed by the mixed-effects modeling. A biophase function of the Sephadex time course was inferred from the modeled eosinophil time courses. In Case Study 2, a mouse model showed that the time course of cytokine-induced $IL_{1\beta}$ challenge was altered with or without drug intervention. Anakinra reversed the $IL_{1\beta}$ induced cytokine IL_6 response in a dose-dependent manner. This Case Study contained time courses of test compound (drug), challenger ($IL_{1\beta}$) and cytokine response (IL_6), which resulted in high parameter precision. Case Study 3 illustrates collagen-induced arthritis progression in the rat. Swelling scores (based on severity of hind paw swelling) were used to describe arthritis progression after the challenge and the inhibitory effect of two doses of an orally administered test compound. In Case Study 4, a cynomolgus monkey model for lipopolysaccharide LPS-induced TNF_α synthesis and/or release was investigated. This model provides integrated information on pharmacokinetics and *in vivo* potency of the test compounds. Case Study 5 contains data from an oral glucose tolerance test in rats, where the challenger is the same as the pharmacodynamic response biomarker (glucose). It is therefore convenient to model the extra input of glucose simultaneously with baseline data and during intervention of a glucose-lowering compound at different dose levels.

* Corresponding author.
E-mail address: Johan.Gabrielsson@slu.se (J. Gabrielsson).
[1] Current address: PharmaLot Consulting AB (Inc.), S-434 92 Vallda, Sweden.

http://dx.doi.org/10.1016/j.ejps.2014.11.006
0928-0987/

Typically time-series analyses of challenger- and biomarker-time data are necessary if an accurate and precise estimate of the pharmacodynamic properties of a test compound is sought. Erosion of data, resulting in the single-point assessment of drug action after a challenge test, should generally be avoided. This is particularly relevant for situations where one expects time-curve shifts, tolerance/rebound, impact of disease, or hormetic concentration–response relationships to occur.

1. Introduction

Ever since the beginning of modern pharmacology, scientists have sought to create animal models for use in translational research to address various disturbances in bodily function. *In vivo* disease models include basically any imaginable variable for a wide array of physiological, (neuro)endocrine, neurological, psychological, and other disorders. Symptoms or syndromes have been introduced in otherwise healthy animals or strains by various means: acute or chronic treatment with pharmacological or chemical/toxicological agents, chemical, mechanical or other lesion-inducing techniques, genetic or inducible knockout technologies, not to mention a variety of behavioral induction procedures (*e.g.*, environmental, cognitive, stress), or even diet-induced aberrations. Some of these approaches have been very successful, others less so. In this paper, we focus on examples of animal models of disease involving pharmacological and/or patho/physiological interaction challenges.

The 'challenge' design is a central theme in many pharmacological studies in which the pharmacodynamic (PD) outcome of provocation is modified by intervention with a test compound ('*x*, *y* . . .', etc.). Such studies are found across various indications, including respiratory disease (Sephadex-induced eosinophil count), arthritis (collagen-induced paw swelling), inflammation (LPS- or $IL_{1\beta}$-induced TNF_{α} or IL_6 biomarker responses), diabetes (blood-glucose handling after intravenous or oral glucose doses), and the central nervous system (seizure thresholds using pentylenetetrazol), to mention just a few (Källstrom et al., 1985; Luross and Williams, 2001; Haddad et al., 2002; Homayoun et al., 2002; Hegen et al., 2008; Lon et al., 2012; Lon et al., 2013; Nolan et al., 2013; Pacini et al., 2013). A challenge design obviously has utility not only for the primary, desired PD action, but also to define the propensity for safety-related PD readouts in the profile of a select agent. In turn, a robust understanding of the safety margins for a novel candidate therapeutic is vitally important for its potential clinical usefulness, *i.e.*, benefit/risk ratio.

The challenge design is sometimes aimed at *acutely* mimicking a *chronic* disease scenario. Sometimes the test compound is already present when the challenge begins, whereas other times, it is administered post-challenge (Bueters et al., 2009). The variability in PD outcome variables is sometimes large or uncontrolled (*cf.* Case Study 1). This is often tackled by increasing the number of measurements (n). Still, many reports rely on a single time-point design, scarce or suboptimal data, or fail to account for hormetic concentration–response relationships with regard to compound ranking. Important/pivotal determinants of a successful quantitative design and analysis are:

- Adequate test compound dose/concentration range (that separates the biomarker response efficiently).
- Adequate challenge dose/concentration (that results in a continuous, robust, repeatable and realistic biomarker response-time course).
- Well-spaced biomarker response – both time- and amplitude-wise.
- Information on the lack or presence of hormetic concentration–response relationships (*i.e.*, a non-monotonic concentration response with specific response features, *e.g.*, a J/U-shaped or inverted U-shaped concentration response; *cf.* Calabrese, 2013).

Therefore, examples of challenge tests are given schematically in Case Studies 1–5 (Fig. 1). Case Study 1 (Sephadex challenge on eosinophil biomarker response) includes vehicle control data containing and reflecting basic handling and procedural stress, but no test compound intervention. Case Study 2 has several time courses of test compound and a full challenge time course of $IL_{1\beta}$ and the IL_6 biomarker response. Case Study 3 contains several time courses of test compound and accompanying time courses of the biomarker (swelling score) with and without test compound, but lacks information about the time course of the challenger (Freund's adjuvant). Case Study 4 covers several time courses of test compound and corresponding time courses of the biomarker response (TNF_{α}), but no information about the challenger (lipopolysaccharide; LPS). Case Study 5 is the oral glucose tolerance test (OGTT) and comprises several time courses of test compound, as well as blood glucose response in vehicle control and test compound groups. In Case Study 5, the levels of the challenger agent (glucose) also represent the actual PD biomarker readout, and the time courses of the challenger and the biomarker response are thus identical.

We will demonstrate some of the issues related to modeling the different kinds of setup. To illustrate the pivotal parts we first characterize the plasma time-course of the test compound, when available (Case Studies 2–5). Then we characterize the time-course of challenger (Case Studies 2 and 5, *e.g.*, $IL_{1\beta}$). If the challenger is not (or cannot be) measured, a biophase function has to be estimated (Case Studies 1, 3 and 4). Finally, the time-course of the pivotal PD biomarker response (Case Studies 1–5, *e.g.*, IL_6) is studied at baseline and after combinations of challenger in the presence or absence of test compound intervention (Fig. 1).

2. Case Study descriptions

The five Case Studies represent different pharmacological *in vivo* models with varying information content from a quantitative modeling point of view. Fig. 1 and Table 1 summarize the availability of data and the particular characteristics of each Case.

2.1. Case Study 1: challenger time-course unknown, no drug intervention

2.1.1. Rationale

The intratracheal (i.t.) rat Sephadex model is a model of acute airway inflammation, with a response dominated by eosinophils. The model has been used to screen drugs for treating asthma (Bondesson, 1997; Evaldsson et al., 2011). Accordingly, Sephadex-induced eosinophilia has been shown to be reduced by pretreatment with budesonide (Källstrom et al., 1985).

Case Study 1 (Fig. 2) illustrates how eosinophils increase in the bronchoalveolar fluid collected by bronchoalveolar lavage (BAL) following i.t. administration of Sephadex as a challenge agent (Källstrom et al., 1985; Haddad et al., 2002). Samples are collected at different time-points after the Sephadex challenge and the number of eosinophils in bronchoalveolar fluid (BAL) is recorded. However, as this PD biomarker response must be obtained post-mortem, it follows that data from each rat by necessity represents

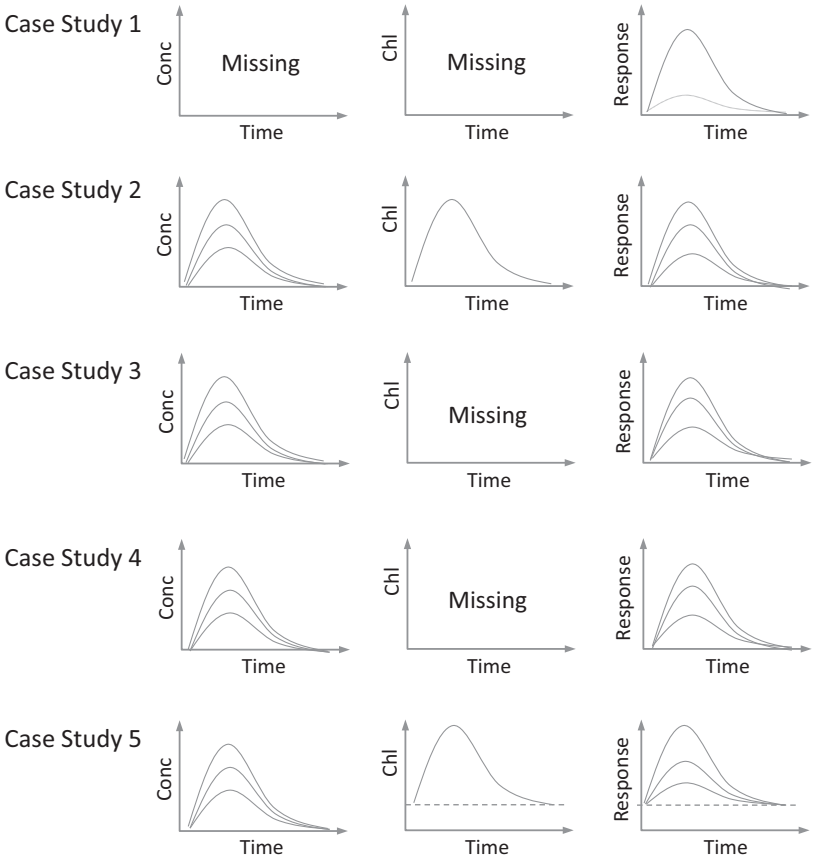

Fig. 1. Schematic diagram of the selection, design and diversity of the five Case Studies used in this report. The left-hand column of concentration–time graphs symbolizes the availability (or not) of test compound plasma concentrations. The middle row time-plots symbolize availability (or not) of the plasma challenger time course. The right hand column of time-plots represents availability of the biomarker response *R* used to evaluate the pharmacodynamic (PD) properties of the test compound.

Table 1
Overview of experimental designs of the five Case Studies including challenge compounds, test compounds and PD biomarker responses.

Case Study	Challenge compound	Animal model	Test compound	PD effect biomarker	Comments
1	Sephadex	Rat	–	Eosinophil count	Lacks challenger time course(s); destructive sampling design; no drug intervention
2	$IL_{1\beta}$	Mouse	Anakinra	IL_6	Includes challenger, test compound, as well as PD response time courses
3	Collagen	Rat	Compound X	Paw swelling	Lacks challenger time courses
4	Lipopolysaccharide	Monkey	Compound Y	TNF_α	Lacks challenger time courses
5	Glucose	Rat	Compound Z	Glucose	Oral glucose tolerance test OGTT model; challenger and PD biomarker identical

a single time-point only. This Case Study represents a mixed-effects modeling approach in drug discovery when data are obtained from destructive sampling. The intent was to quantify the turnover of eosinophils triggered by a Sephadex challenge in the absence of a time-course of the latter.

2.1.2. Materials and methods

2.1.2.1. Chemicals. Sephadex G-100 Superfine (Sigma–Aldrich, Sweden) was dissolved in physiological saline (9 mg mL^{-1} NaCl) to a final concentration of 10 mg mL^{-1}. The solution was prepared 2 h prior to administration.

2.1.2.2. Animals. Healthy male non-fasted Sprague–Dawley rats (226–250 g, Charles River) were used. Data were collected from a total of 268 animals from 4 separate studies.

2.1.2.3. In vivo model. The rats were lightly anaesthetized (2–3 min, 4% isoflurane in O_2) and placed in a supine position. Sephadex (10 mg mL^{-1}) was administered intra-tracheally at a volume of 200 μL per rat. The rats were returned to their cages in an upright position.

Individual rats were euthanized with an intraperitoneal injection of 1.0 mL pentobarbital (60 mg mL^{-1}, Apoteksbolaget, Sweden) at different times up to 1 week after dosing. The trachea was exposed and a syringe connected to a polyethylene tube (PE120) was inserted into the trachea through a cut between two upper cartilage rings. The tube was secured with a silk suture. Lavage of the lungs was done manually using a volume of 4 mL of RT PBS (w/o Ca^{2+} and Mg^{2+}) in a 2× in/2× out manner. The obtained BAL fluid was centrifuged (Sorvall Rotanta 46R, 1200 rpm, 10 min, 4 °C). The pellet was re-suspended in 0.5 mL of PBS and the total and differential cell count was performed using a SYSMEX XT-1800i Vet. (SYSMEX, Kobe Japan).

2.1.2.4. Pharmacokinetic and pharmacodynamic methods. Population fitting was performed using the Pharsight Phoenix 6.2.0. The

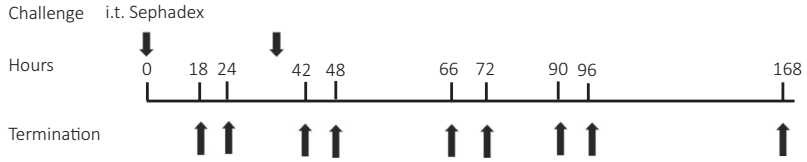

Fig. 2. Schematic presentation of the design of Case Study 1. Arrows indicate approximate time points of eosinophil assessment.

concentration of Sephadex in the lungs was unknown. The time-course of the challenge function S(Sephadex) was therefore inferred from biomarker data and modeled as such

$$S_{\text{Sephadex}}(t) = A_1 \cdot K_{p1} \cdot t \cdot e^{-K_{p1} \cdot t} \quad (1:1)$$

where A_1, K_{p1} and t stand for the amplitude, rate constant, and time, respectively, of the stimulatory function resulting from the Sephadex challenge. A separate function due to the stimulatory action of procedural stress S(Stress) that is also part of the non-drug vehicle control PD response to Sephadex was modeled as

$$S_{\text{Stress}}(t) = A_2 \cdot K_{p2} \cdot t \cdot e^{-K_{p2} \cdot t} \quad (1:2)$$

where A_2 and K_{p2} represent the amplitude and rate constant, respectively, of the stimulatory function due to procedural stress. The resulting eosinophil count in bronchoalveolar fluid then becomes

$$\frac{dR}{dt} = R_0 \cdot k_{out} \cdot (1 + S_{\text{Sephadex}}(t) + S_{\text{Stress}}(t)) - k_{out} \cdot R \quad (1:3)$$

where R, R_0 and k_{out} are the number of eosinophils, the predicted number of eosinophils at the time of challenge and the fractional turnover rate of eosinophils, respectively. Eq. (1:4) gives the relationship of the PD biomarker response R (eosinophil number) at different levels of stress/Sephadex challenge.

$$R = R_0 \cdot (1 + S(\text{Sephadex}) + S(\text{Stress})) \quad (1:4)$$

2.1.2.5. Numerics. PhoenixWinNonlin 6.3, with a Gauss–Newton (Levenberg and Hartley) differential equation solver, was used for both simulating and regressing data. A constant CV (proportional error) model was used as weighting function. All biomarker-time courses were simultaneously regressed, and data from different study dates were combined in the final analysis.

2.1.3. Results and discussion

The primary objective of this first model was to characterize the time-profile of the response to Sephadex and subsequently define the underlying biophase function of the challenger 'driving' the response in eosinophils. To fully understand test compound-biomarker response, we suggest that both the test compound exposure and the underlying inflammatory response (biophase function) driving the eosinophilia be verified experimentally.

In Case Study 1, eosinophilia occurred at similar time-points following Sephadex challenge as previously reported (Haddad et al., 2002), peaking at about 48 h and slowly declining 72 h post 5 mg/kg Sephadex i.t. dosing (Fig. 3). The decline in eosinophilia was much slower than the predicted increase and elimination of Sephadex (biophase function), and was still measurable up to a week after challenge (animal ethical constraints prohibited following the full return of the eosinophilia response to baseline). Therefore, it was still possible to fit the proposed model (Eq. (1:3)) to experimental data and obtain parameter estimates with reasonable precision. The underlying Sephadex biophase function (Eq. (1:1)) peaked within 24 h of starting the challenge, in contrast to the maximum eosinophil count (>50 h). The vehicle-induced stress/handling effect contributed marginally to the biomarker response (Table 2) (see Fig. 4).

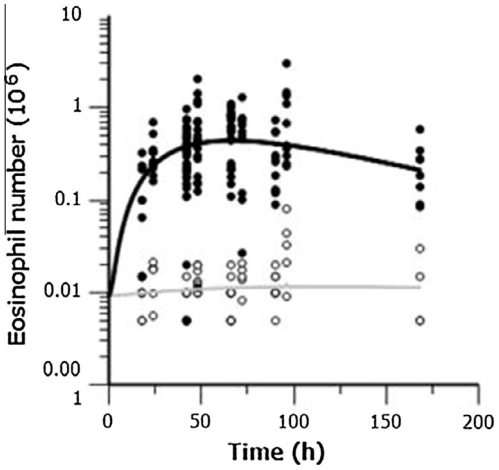

Fig. 3. Number of eosinophils in individual rats at different times of termination, given Sephadex (filled circles) or vehicle (open circles). Lines describe the mean predicted number of eosinophils for rats treated with vehicle (bottom) or Sephadex (upper), respectively.

2.2. Case Study 2: compound, challenger and PD response time-courses known

2.2.1. Rationale

The overall objective in Case Study 2 (Fig. 5), a mouse model, was to create an acute *in vivo* challenge model for evaluation of new human interleukin-1 (IL_1) receptor antagonist (IL_{1Ra}) candidates. Anakinra (Kineret®) is a recombinant, non-glycosylated human IL_{1Ra} that antagonizes the effects of both $IL_{1\alpha}$ and $IL_{1\beta}$ by blocking the binding of IL_1 to cell surface receptors, and that has protective effects against several IL_1-mediated pathological processes, such as septic shock, inflammatory bowel disease, and others (Eder, 2009). It was thus used as a positive benchmarking compound in this study. The time courses of Anakinra and of the challenger $IL_{1\beta}$ were evaluated first. Based on these results, IL_6 biomarker response-time courses were collected, with injections of Anakinra given 30 min before the challenger $IL_{1\beta}$. Individual challenge data were then used as critical input to assess the individual biomarker response IL_6.

2.2.2. Methods

2.2.2.1. Chemicals and reagents. Recombinant mouse $IL_{1\beta}$ ($mIL_{1\beta}$; R&D systems, 401-ML, 25 μg *E. coli* derived) and Anakinra

Table 2
Final Sephadex parameter estimates and their precision (CV%).

Parameter	Units	Estimate	CV%
K_{p1}	h^{-1}	0.0507	18
K_{p2}	h^{-1}	0.106	38
A_1		337.	23
A_2		1.21	20
k_{out}	h^{-1}	0.011	26
R_0		0.0093	

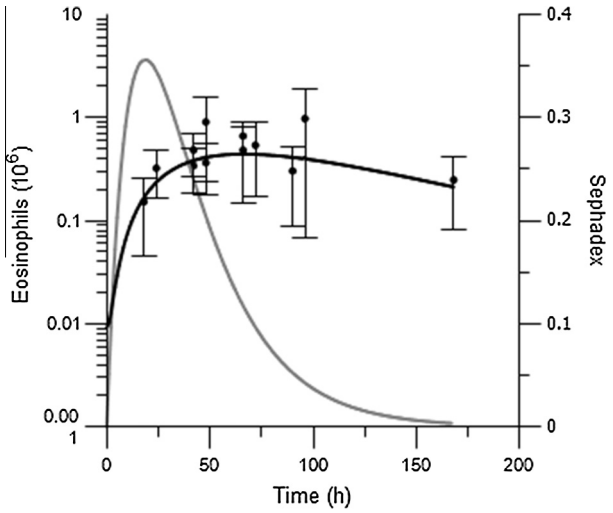

Fig. 4. Experimental (filled circles and error bars and left-hand axis) and model predicted (thick solid line and left-hand axis) number of eosinophils in rats treated with Sephadex. The thin black line (peak time t_{max} at 24 h) is the predicted Sephadex biophase function (Eq. (1:1) and right hand axis).

(Kineret® 100 mg, Anakinra Amgen Europe B.V.), were used as challenge and intervention compounds, respectively, in the *in vivo* challenge mouse model.

2.2.2.2. Animals. Healthy Balb/c mice (7–8 weeks old; males, Charles River), non-fasted, with a minimum body weight of 20 g, were used in the $IL_{1\beta}$ induced cytokine release model with or without intervention with Anakinra.

2.2.2.3. In vivo model of $IL_{1\beta}$-induced cytokine release. A PD model was designed to characterize the time course of cytokine release following $IL_{1\beta}$ challenge, with or without drug intervention. The mice were randomly divided into four treatment groups, to receive either one single intraperitoneal (i.p.) dose of Anakinra 0.4 mg kg^{-1}, 2 mg kg^{-1}, or 10 mg kg^{-1}, respectively, or saline, with a dose volume of 10 mL kg^{-1}. Different doses of Anakinra or saline were injected 30 min before administration of the challenger $IL_{1\beta}$ (133 ng). Mice were sacrificed at each of the following time points: 0, 0.5, 2, 4 and 8 h post $IL_{1\beta}$ challenge, with groups of three mice (Fig. 6). Mice were anesthetized with isoflurane (Forene,® Abbott Scandinavia, Sweden) and blood was collected via heart puncture for challenge ($IL_{1\beta}$), PK (Anakinra) and PD biomarker (IL_6) analysis. The plasma samples were centrifuged at 10,000*g* for 5 min at 4 °C and stored in plastic Eppendorf tubes placed on ice during handling and kept at −80 °C pending quantification.

2.2.2.4. Bioanalysis of test compound. A sandwich ELISA was qualified to measure levels of Anakinra in mouse plasma samples using the duo set antibody pair from R&D Systems (Abingdon, UK). Briefly, the capture monoclonal antibody (10 μg mL^{-1}), specific

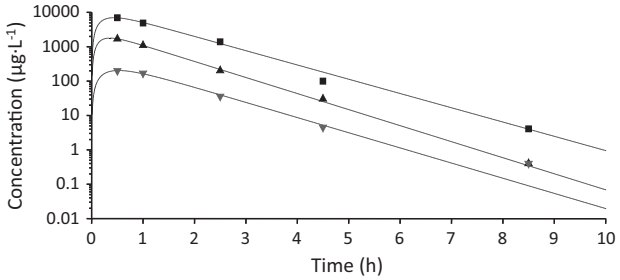

Fig. 6. Semilogarithmic plot of Anakinra concentration–time data of experimental (symbols) and model predictions (solid lines) after subcutaneous doses of Anakinra at 0.4 mg kg^{-1} (solid down-triangles), 2 mg kg^{-1} (solid up-triangles) and 10 mg kg^{-1} (solid squares), respectively (mean values, $n = 3$).

for human IL_{1Ra} (Ra = receptor antagonist), was coated onto the wells of the microtiter plates (Nunc Immunomodule, C8 maxi immunomodule #145–445101). Samples, including standards (40–2500 pg mL^{-1}) of known human IL_{1Ra} content, controls, and unknowns, diluted in 1% BSA in PBS, were added into these wells and incubated. After washing, a biotinylated goat-anti-human IL_{1Ra} was used as detecting antibody. Then streptavidin conjugated with HRP was added and tetramethyl benzidine (TMB) was used as substrate. No cross-reactivity was obtained with mouse IL_{1Ra}. Plasma matrix effects were observed, and therefore standards/controls were diluted exactly as the unknown plasma samples. IL_6 and $IL_{1\beta}$ were analyzed using the Bioplex mouse cytokine assays (Bio-rad) according to the manufacturer's instruction.

2.2.2.5. Pharmacokinetic and pharmacodynamic methods. The Anakinra time course C_i in plasma upon repeated dosing was captured by Eq. (2:1)

$$C_i = A \cdot (e^{-K \cdot t} - e^{-K_a \cdot t}) \quad (2:1)$$

where A, K and K_a are the kinetic parameters allowing a smooth representation of the Anakinra concentration–time course in plasma. The time course of challenger $IL_{1\beta}$ in plasma upon repeated dosing was captured by Eq. (2:2)

$$C_{IL_{1\beta}} = S \cdot (e^{-K \cdot t} - e^{-K_a \cdot t}) + C_{IL_{1\beta}}(\text{baseline}) \quad (2:2)$$

where S, K and K_a are the kinetic parameters allowing a smooth representation of the $IL_{1\beta}$ concentration–time course in plasma. The stimulatory impact of $IL_{1\beta}$ on the time-course of IL_6 is modeled via a series of transduction steps as follows

$$\begin{aligned} &\frac{dR_1}{dt} = k_{in} \cdot S(C_{IL_{1\beta}}) - k_{out} \cdot R_1 \\ &\cdots \\ &\frac{dR_n}{dt} = k_{out} \cdot R_{n-1} - k_{out} \cdot R_n \end{aligned} \quad (2:3)$$

where k_{in}, $S(C_{IL_{1\beta}})$ and k_{out} are the turnover rate, the $IL_{1\beta}$ stimulatory function and the fractional turnover rate, respectively. The stimulatory function $S(C_{IL_{1\beta}})$ is mathematically written as a linear function of the $IL_{1\beta}$ exposure

$$S(C_{IL_{1\beta}}) = 1 + P \cdot (C_{IL_{1\beta}} - C_{IL_{1\beta}}(\text{baseline})) \quad (2:4)$$

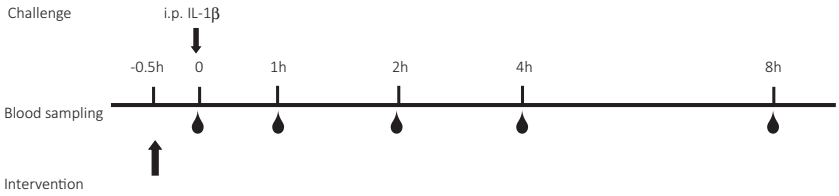

Fig. 5. Schematic presentation of Case Study 2 design. A range of doses of Anakinra or physiological NaCl (control) were injected 30 min before administration of the challenger $IL_{1\beta}$ (133 ng). Groups of three mice were sacrificed at each time point (0, 1, 2, 4 and 8 h) post $IL_{1\beta}$ challenge.

where P is a pharmacodynamic parameter (IL_6 increase) and $\Delta IL_{1\beta}$ is the change from $IL_{1\beta}$ baseline caused by the $IL_{1\beta}$ challenge. The inhibitory action of Anakinra on $IL_{1\beta}$ is given by Eq. (2:5)

$$S(C_{IL_{1\beta}}, C_i) = 1 + P \cdot (C_{IL_{1\beta}} - C_{IL_{1\beta}}(\text{baseline})) \cdot I(C_i) \quad (2:5)$$

where the inhibitory Anakinra function $I(C_i)$, assumed to impact the change of $IL_{1\beta}$ from its baseline value, is given by Eq. (2:6) as

$$I(C_i) = 1 - \frac{C_i}{IC_{50,i} + C_i} \quad (2:6)$$

$IC_{50,i}$ is the potency value of Anakinra at the $IL_{1\beta}$ receptor. Eq. (2:7) gives the relationship of the biomarker response R and different levels of drug intervention on the $IL_{1\beta}$ challenge.

$$R = R_0 \cdot S(C_{IL_{1\beta}}, C_i) = R_0 \cdot \left(1 + P \cdot \left(C_{IL_{1\beta}} - C_{IL_{1\beta}}(\text{baseline})\right) \cdot \left(1 - \frac{C_i}{IC_{50,i} + C_i}\right)\right) \quad (2:7)$$

2.2.2.6. Numerics. WinNonlin 5.2, with a Runge–Kutta–Fehlberg differential equation solver, was used for both simulating and regressing data. A constant CV (proportional error) model was used as weighting function. All biomarker-time courses were simultaneously regressed.

2.2.3. Results and discussion

The objective of Case Study 2 was to set up an acute *in vivo* challenge model for kinetic/dynamic evaluation of novel IL_1 receptor antagonists (IL_{1Ra}) according to the design in Fig. 5. A one-compartment pharmacokinetic model was fitted to Anakinra concentration–time data from each of the three dose groups (Eq. (2:1), Fig. 6 and Table 3). This served as a smoothing function and input to Eq. (2:5). The results showed that the time course of cytokine response (IL_6) induced by $IL_{1\beta}$ challenge in the mouse was suppressed with Anakinra intervention in a dose-dependent manner. This Case Study contained time courses of test compound (drug), challenger ($IL_{1\beta}$) as well as cytokine response (IL_6). Experimental and model-predicted data were consistent (based on mean values in the study) for Anakinra concentrations, challenger $IL_{1\beta}$ and biomarker response IL_6 (Fig. 7).

The time courses of the challenger $IL_{1\beta}$ were evaluated as a control in the three Anakinra dose groups and in the vehicle control group, respectively (Fig. 7). The time courses of $IL_{1\beta}$ overlapped in all challenge treatment groups. $IL_{1\beta}$ was modeled with a first-order absorption and elimination process (Eq. (2:2)) using a fixed baseline value R_0 of $IL_{1\beta}$ (R_0 used as a constant and set at 43 ng L^{-1}). The $IL_{1\beta}$ parameters were estimated based on mean values from all for treatment groups with low variability <10% (Table 4).

Finally the time course of the biomarker IL_6 was measured at baseline and after challenges of $IL_{1\beta}$ with or without Anakinra intervention (Fig. 8). The inhibitory action by Anakinra was defined by Eq. (2:5). All dose groups were fitted simultaneously and the final parameter estimates had an acceptable precision as judged from the relative standard deviation (CV < 20%, Table 5). An exposure-dependent IL-6 response was established in the mouse model with an IC_{50} of 16 μg L^{-1} *in vivo* compared with the IC_{50} of 2 μg L^{-1} *in vitro* (Fredericks et al., 2004).

Table 3
Final Anakinra exposure parameter estimates and their precision (CV%).

Dose (mg kg^{-1})	Parameter	Units	Estimate	CV%
0.4	A	μg L^{-1}	507	30
	K_a	h^{-1}	3.2	30
	K	h^{-1}	1.0	10
2	A	μg L^{-1}	3210	7
	K_a	h^{-1}	5.8	20
	K	h^{-1}	1.1	4
10	A	μg L^{-1}	13,550	20
	K_a	h^{-1}	4.5	40
	K	h^{-1}	1.9	10

2.3. Case Study 3: challenger time course unknown

2.3.1. Rationale

Rheumatoid arthritis (RA) is a chronic, immune-mediated inflammatory disease characterized by joint swelling, synovial tissue inflammation and subsequent damage to the cartilage (Beevart et al., 2010; Brooks, 2006). The collagen-induced arthritis (CIA) model (Fig. 9) in the rat is frequently used to mimic RA disease progression in a short time frame and to test the efficacy of novel anti-arthritic drug candidates (Hegen et al., 2008).

2.3.2. Methods

2.3.2.1. Chemicals and reagents. Porcine collagen type II in 0.05 M acetic acid (2 mg mL^{-1}, Chondrex Inc., Redmond, USA) was slowly emulsified on ice with incomplete Freund's adjuvant (1:1 v/v) (BD Difco, Detroit, USA) by adding the collagen drop-wise to the incomplete Freund's adjuvant while mixing. The arthritis-inducing emulsion was prepared immediately before immunization. The test drug was dissolved at concentrations of 2 mg mL^{-1} and 6 mg mL^{-1} in 0.5% carboxymethyl cellulose (Sigma Aldrich)/0.5% Tween80 (Sigma Aldrich). The dosing solution was prepared fresh daily on the day of dosing.

2.3.2.2. Animals. Healthy female Lewis rats (Janvier Labs, France) with a body weight of 140–160 g were used in the CIA studies. The animals were housed in groups of three and had free access to rat chow and water.

2.3.2.3. CIA induction and treatment studies. Rats were immunized with 0.2 mL (200 μg) of the collagen emulsion by intradermal (i.d.) injection into the base of the tail under isoflurane anesthesia (Forene®, Abbott Scandinavia, Sweden). A booster injection (i.d.) with 0.1 mL (100 μg) emulsion was given 7 days after immunization.

After evaluation of paw edema induction on day 16, 15 CIA rats with paw size increases of at least 50% in one or two paws were selected. The rats were randomly assigned to one of three treatment groups, to receive oral doses of 10 mg kg^{-1} or 30 mg kg^{-1} of the test drug, or vehicle, respectively, with dose volumes of 5 mL kg^{-1}. The animals were dosed on day 16 post-induction and were treated daily with test compound until day 34 post-induction. Serial EDTA blood samples were collected from the sublingual vein on day 2 (2, 4, 8, 22 h) and day 19 (2, 4, 8, 27 or 28 h) after oral dosing of test compound. The blood samples were

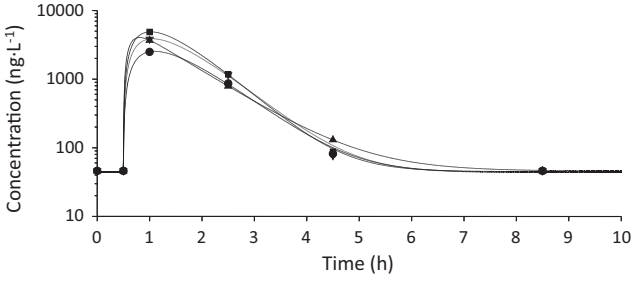

Fig. 7. Semilogarithmic plot of $IL_{1\beta}$ concentration–time data of experimental (symbols) and model predictions (solid lines) after an intraperitoneal challenge dose of 133 ng $IL_{1\beta}$ in mice (mean values where $n = 3$).

Table 4
Final challenge ($IL_{1\beta}$) parameter estimates and their precision (CV%).

Parameter	Units	Estimate	CV%
S		6580	2
K_a	h^{-1}	7.2	6
K	h^{-1}	1.1	1
R_0	$ng\ L^{-1}$	45.7	1

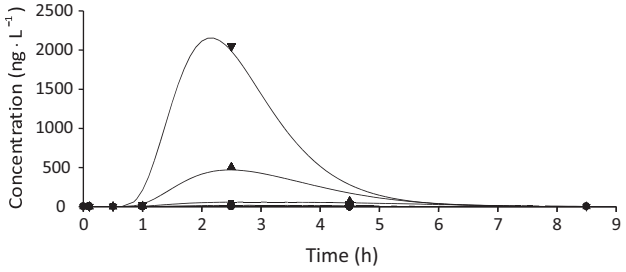

Fig. 8. Semilogarithmic plot of IL_6 concentration–time data of experimental (symbols) and model predictions (solid lines) after an intraperitoneal challenge dose of 133 ng $IL_{1\beta}$ to mice (mean values where $n = 3$) and different doses of Anakinra at 0 mg kg^{-1} (solid down triangles), 0.4 mg kg^{-1} (solid up triangles), 2 mg kg^{-1} (solid squares), 10 mg kg^{-1} (solid circles), respectively.

Table 5
Final IL_6 biomarker parameter estimates and their precision (CV%).

Parameter	Units	Estimate	CV%
k_{out}	h^{-1}	4.3	10
IC_{50}	$\mu g\ L^{-1}$	16	20
R_0	$ng\ L^{-1}$	0.8	4

stored in plastic Eppendorf tubes, placed on ice during handling and kept at −20 °C until analysis of the test compound.

2.3.2.4. Drug analysis. The test compound was quantified in rat blood using a sensitive and specific LC–MS/MS method.

2.3.2.5. Assessment of arthritis swelling score. The incidence and severity of CIA was evaluated using an arthritis scoring system. Hind-paw swelling was scored on a composite scale of 0–12 per rat, evaluating each paw in the metatarsal region with score 0–3 and in the ankle with score 0–3, thus obtaining a maximal score of 6 per paw. The total arthritis scores were calculated from the sum of both hind paws, with a maximum possible score of 12 for each rat. The following scoring system was used: 0 = no detectable sign of inflammation; 1 = light swollen region; 2 = more obviously swollen region; 3 = ankylosis or severely swollen region.

2.3.2.6. Pharmacokinetic and pharmacodynamic methods. The time course in blood upon repeated daily oral dosing of the CIA-modifying test compound was described by Eq. (3:1)

$$C = \frac{dose \cdot K_a}{V \cdot (K_a - K)} \cdot (e^{-K \cdot t} - e^{-K_a \cdot t}) \quad (3:1)$$

where V/F, K and K_a are the kinetic parameters allowing a smooth representation of test compound concentration–time course in plasma. The stimulatory impact of collagen on the time-course of paw swelling (swelling scores) was modeled by means of series of transduction steps as follows

$$\left.\begin{aligned} \tfrac{dR_1}{dt} &= k_{out} \cdot (\Delta R - R_1) \\ \tfrac{dR_2}{dt} &= k_{out} \cdot (R_1 - R_2) \\ \tfrac{dR_3}{dt} &= k_{out} \cdot (R_2 - R_3) \\ \tfrac{dR_4}{dt} &= k_{out} \cdot (R_3 - R_4) \\ \tfrac{dR}{dt} &= k_{in}(t) \cdot R_4 - k_{out} \cdot R \end{aligned}\right\} \quad (3:2)$$

where k_{out} is the fractional turnover rate, $k_{in}(t)$ the time-dependent turnover rate, and the ΔR parameter, the difference between the baseline swelling score R_0 and R_{max}. $k_{in}(t)$, was mathematically described by Lon et al. (2011) as a function of time which was dependent on the degree of swelling

$$\frac{dk_{in}(t)}{dt} = -R_{deg} \cdot k_{in} \quad (3:3)$$

R_{deg} is a first-order rate constant which describes a negative feedback loop (Earp et al., 2008a, 2008b). The inhibitory action caused by the test compound was defined by Eq. (3:4) as

$$I(C_i) = 1 - \frac{I_{max} \cdot IC_{50,i}^n}{IC_{50,i}^n + C_i^n} \quad (3:4)$$

where $IC_{50,i}$ is the potency value of the test item at the relevant target in question. The combined effects of Eqs. 3:2, 3:3, 3:4 are shown in Eq. (3:5)

$$\frac{dR_n}{dt} = k_{in}(t) \cdot R_{n-1} \cdot I(C_i) - k_{out} \cdot R_n \quad (3:5)$$

Eq. (3:6) gives the time-dependent relationship of the PD biomarker R (swelling score) and different levels of test compound intervention.

$$R = \frac{k_{in}(t)}{k_{out}} \cdot I(C_i) = R_0(t) \cdot \left(1 - \frac{I_{max} \cdot C_i^n}{IC_{50}^n + C_i^n}\right) \quad (3:6)$$

2.3.2.7. Numerics. PhoenixWinNonlin 6.3, with a Gauss–Newton (Levenberg and Hartley) differential equation solver, was used for simulating and regressing data. A constant CV (proportional error) model was used as a weighting function. All swelling score time courses were simultaneously regressed.

2.3.3. Results and discussion

The objective of Case Study 3 was to set up a quantitative model to describe the time course of collagen-induced arthritis with and without test compound intervention in the rat. Following stimulation with collagen the onset of arthritis occurred with a

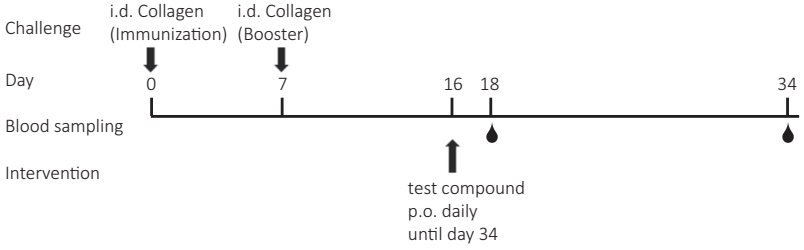

Fig. 9. Schematic presentation of the design of Case Study 3. Arthritis was induced by intradermal collagen injections on day 0 and day 7. The test drug was administered orally at three different doses (0 mg kg^{-1} – *i.e.* vehicle control – 10 mg kg^{-1} and 30 mg kg^{-1}) over 19 consecutive days starting on day 16 after the collagen challenge started.

12-day delay post-immunization and with a mean peak onset at day 24.

A one-compartment pharmacokinetic model (Eq. (3:1)) was fitted to the mean test drug concentration–time data of the two dose groups (Fig. 10 and Table 6). This served as input to the inhibitory drug-mechanism function Eq. (3:5).

All groups were fitted simultaneously using a 4-transit-compartment driven turnover model (Eqs. 3:2, 3:3, 3:4). The final parameter estimates had good precision (CV < 10%; Table 7). Mean experimental and model predicted data were consistent for test compound concentrations and biomarker swelling scores (Figs. 10 and 11). The half-lives of the swelling-score ($t_{1/2kout}$) and the first-order degradation parameter R_{deg} of the turnover rate ($t_{1/2Rdeg}$) were approximately 2 and 30 days, respectively.

The inhibitory effect of the test compound on CIA was characterized with a potency value IC_{50} of 74 μg L^{-1} *in vivo*. Since the efficacy of the test compound was estimated to 0.99, this suggests that an approximation to unity (1) would be also applicable. The high Hill-factor n indicates an almost dichotomous concentration–response relationship.

2.4. Case Study 4: test compound time-course known

2.4.1. Rationale

LPS-induced cytokine release in cynomolgus monkeys has been used to test effects of drugs against inflammation in acute disease conditions (*e.g.*, Mitchell et al., 2010; Wang et al., 2007). We constructed a PD biomarker response model based on the time course of LPS-induced TNF_α release with or without inhibitory test compound intervention in this species (Fig. 12).

2.4.2. Methods

2.4.2.1. Chemicals and reagents. LPS (*E. coli* 055:B5, Sigma), Polyethylene glycol 200 (Fluka), Solutol HS 15 (BASF Pharma solutions), citric acid anhydrous (Sigma, C-1857) were used.

2.4.2.2. Animals. Healthy cynomolgus monkeys aged 10–11 years (mean body weight of all test animals was 6.6 kg; females: 4.5–6.2 kg, males: 7.2–9.1 kg) were used in this LPS-induced cytokine release study with or without the administration of test compound.

For this PD biomarker study, two groups were independently treated according to a cross-over design for treatment vs. vehicle, with treatment sessions separated by several days. Each group consisted of four cynomolgus monkeys (two males and two females). The animals were not fasted but no food was supplied during the first 2 h after LPS administration.

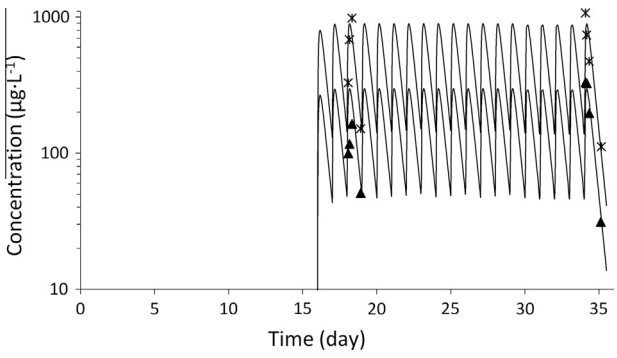

Fig. 10. Semi-logarithmic plot of blood concentration–time data of experimental (symbols) and model predictions (solid lines) after oral doses of the test compound at 10 mg kg^{-1} (up-triangles) and 30 mg kg^{-1} (stars) respectively (n = 5).

Table 6
Kinetic parameter estimates and their precision (CV%).

Parameter	Units	Estimate	CV%
K	d^{-1}	2.5	18
V/F	L	25	25
K_a	d^{-1}	11.7	57

Table 7
Final swelling score parameter estimates and their precision (CV%).

Parameter	Units	Estimate	CV%
R_0	Score	0.39	5
R_{max}	Score	94	10
k_{out}	d^{-1}	0.38	5
R_{deg}	d^{-1}	0.023	3
I_{max}		0.99	4
IC_{50}	μg L^{-1}	74	7
n		5	9

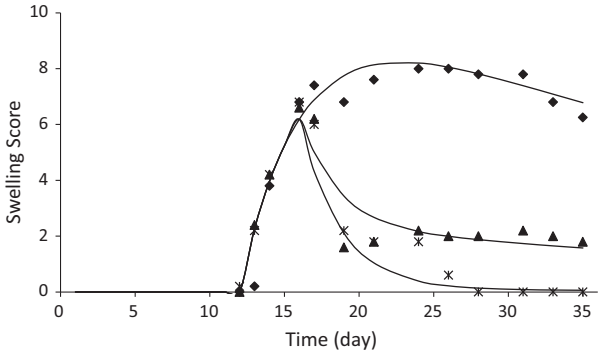

Fig. 11. Plot of swelling score (medians) vs. time data of experimental (symbols) and corresponding model predictions (solid lines) after intradermal challenge with collagen in rats (n = 5) and different doses of the test compound at 0 mg kg^{-1} (vehicle; diamonds), 10 mg kg^{-1} (up triangles) and 30 mg kg^{-1} (stars), respectively.

At the testing session, the monkeys received either test compound or vehicle as an initial i.v. bolus followed by a 1 h infusion. The vehicle was made up from 1 M HCl (2% v/v), polyethylene glycol 200 (10% v/v), solutol HS 15 (10%, v/v) and 100 mM citrate buffer pH3 (78%, v/v). The applied volume of the intravenous bolus was 0.5 mL kg^{-1} and the infused volume rate was 5 mL kg^{-1} h^{-1}. The intravenous bolus and constant-rate infusion doses were 1 mg kg^{-1} and 1 mg kg^{-1} h^{-1} (low dose); 2.9 mg kg^{-1} and 3.1 mg kg^{-1} h^{-1} (high dose); infusion time 1 h. At 0.33 h after infusion of the test compound began, the animals received an intravenous LPS challenge at 1 μg kg^{-1} mL^{-1} in 0.9% NaCl. Venous EDTA-blood was sampled at 0, 0.33, 1, 1.33, 2, 4, 7, and 24 h after treatment began in order to assess test compound exposure, and at 0, 1, 1.33, 2, 4, 7, and 24 h for the biomarker analysis. Samples were stored at −20 °C until analysis.

2.4.2.3. Bioanalysis of test compound concentration. The test compound was quantified in monkey blood by using a sensitive and specific LC–MS/MS method. Lower limit of quantification was at 4 nmol L^{-1} and upper limit of quantification was at 12,000 nmol L^{-1}.

TNF_α was quantified by a non-human primate multiplex kit system (PRCYTOMAG-40K, Millipore) in cynomolgus monkey EDTA plasma samples according to the provider's instructions, using a Luminex Magpix Instrument for magnetic bead-based detection and the MasterPlex QT software (Hitachi Software) for cytokine quantification. All samples were run in duplicate and quantification was based on back-calculation of assay signals to a standard

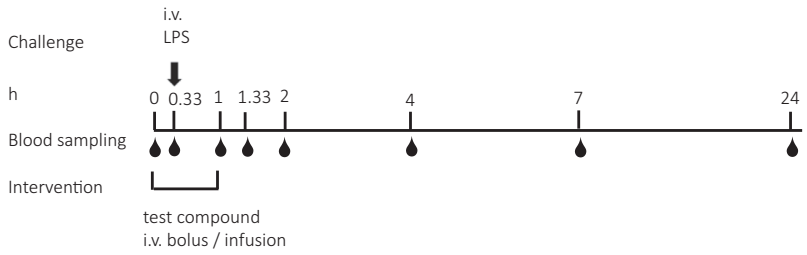

Fig. 12. Schematic presentation of the design of Case Study 4. Starting at t_0, the test item was administered as an iv-bolus followed by a 1 h intravenous infusion. The LPS challenge (1 μg kg^{-1} mL^{-1} in NaCl) was administered intravenously at 0.33 h. Blood sampling for test compound exposure (down triangles) and TNF$_\alpha$ (up triangles) is indicated.

curve with 8 points in a range of 2.4–10,000 pg mL^{-1}. In addition, quality control samples generated by spiking of plasma matrix with defined analyte concentrations were generated with 6 points in the range of 10–5000 pg mL^{-1}. Based on the quality control results, the lower limit of quantification was 10 pg mL^{-1} and the upper limit of quantification was 5000 pg mL^{-1}.

2.4.2.4. Pharmacokinetic and pharmacodynamic methods. The time course of test compound in plasma after the i.v. bolus + constant rate infusion regimen was captured by a two-compartmental model

$$\left.\begin{aligned} V_c \cdot \frac{dC_p}{dt} &= Input_{bolus} + Input_{infusion} - CL \cdot C_p - CL_d \cdot (C_P - C_t) \\ V_t \cdot \frac{dC_t}{dt} &= CL_d \cdot (C_p - C_t) \end{aligned}\right\} \quad (4:1)$$

where $Input_{bolus}$ and $Input_{infusion}$ represent the i.v. bolus dose and i.v. infusion dose, respectively. C_p denotes test compound concentration, CL clearance and V volume of the central compartment. C_t denotes the peripheral concentration, CL_d the inter-compartmental distribution term and V_t the peripheral volume.

The stimulatory impact of LPS on the time-course of TNF$_\alpha$ was described by a turnover model connected to a series of transit compartments

$$\left.\begin{aligned} &\frac{dR_1}{dt} = k_{in} \cdot S(\mathrm{LPS},C_i) - k_{out} \cdot R_1 \\ &\cdots \\ &\frac{dR_n}{dt} = k_{out} \cdot R_{n-1} - k_{out} \cdot R_n \end{aligned}\right\} \quad (4:2)$$

where k_{in} is the turnover rate, S(LPS, C_i) the LPS challenge stimulatory function with or without test compound intervention, and k_{out} the fractional turnover rate. S(LPS, C_i) is mathematically written as an exponential function of time

$$S(\mathrm{LPS},C_i) = 1 + a \cdot k' \cdot t \cdot e^{(-k' \cdot t)} \quad (4:3)$$

where a and k' are pharmacodynamic parameters of LPS stimulation used to describe the TNF$_\alpha$ response. When test compound is given, Eq. (4:3) becomes

$$\left.\begin{aligned} S(\mathrm{LPS},C_i) &= 1 + A \cdot k' \cdot t \cdot e^{(-k' \cdot t)} \cdot I(C_i) \\ S(\mathrm{LPS},C_i) &= (1 + A \cdot k' \cdot t \cdot e^{(-k' \cdot t)}) \cdot I(C_i) \end{aligned}\right\} \quad (4:4)$$

where the inhibitory action of the test compound is assumed to act on the time course of the stimulatory deviation *per se* (upper row in Eq. (4:4)) or on the whole stimulatory function (lower row of Eq. (4:4)). The inhibitory action caused by the test compound $I(C_i)$ is defined by Eq. (4:5) as

$$I(C_i) = 1 - \frac{C_i}{\mathrm{IC}_{50,i} + C_i} \quad (4:5)$$

where $\mathrm{IC}_{50,i}$ is the potency parameter. This relationship assumes a 100% inhibitory action of test compound on the LPS challenge. Eq. (4:6) gives the relationship of the biomarker response R and different levels of test compound intervention on the LPS challenge.

$$\left.\begin{aligned} R = R_0 \cdot S(\mathrm{LPS};C_i) &= R_0 \cdot \left(1 + A \cdot k' \cdot t \cdot e^{(-k' \cdot t)} \cdot \left(1 - \frac{C_i}{\mathrm{IC}_{50} + C_i}\right)\right) \\ R = R_0 \cdot S(\mathrm{LPS};C_i) &= R_0 \cdot \left(1 + A \cdot k' \cdot t \cdot e^{(-k' \cdot t)}\right) \cdot \left(1 - \frac{C_i}{\mathrm{IC}_{50} + C_i}\right) \end{aligned}\right\} \quad (4:6)$$

The larger the test compound exposure, the higher the suppression of LPS stimulation, and the later the biomarker TNF$_\alpha$ peak occurs.

2.4.2.5. Numerics. PhoenixWinNonlin 6.3, with a Gauss–Newton (Levenberg and Hartley) differential equation solver, was used for simulating and regressing data. A constant CV (proportional error) model was used as weighting function for the kinetic data and a constant absolute error model for biomarker data. All biomarker-time courses were simultaneously regressed.

2.4.3. Results and discussion

The objective of Case Study 4 was to quantitatively describe the inhibitory effect of a test compound on TNF$_\alpha$ (the PD biomarker) after LPS was given as an acute immunological challenge. The test compound was administered prophylactically as an intravenous bolus + infusion regimen in order to establish a constant, systemic, test-compound exposure at the time of challenge (LPS administration). A two-compartmental pharmacokinetic model was fitted to the mean test compound concentration–time data from the two dose groups (Eq. (4:1), Table 8, and Fig. 13). This served as a smoothing function and input to Eq. (4:5). The TNF$_\alpha$ PD response was characterized by a rapid increase followed by a rapid drop (Fig. 14, left). The TNF$_\alpha$ baseline response was obtained from the vehicle-treated animals (Fig. 14). A turnover model for TNF$_\alpha$ levels was established incorporating a time-dependent stimulatory function acting on k_{in} to capture the stimulatory impact of LPS challenge (Eq. (4:2)). TNF$_\alpha$ levels drop below the baseline causing a rebound-phenomenon if the inhibition is allowed to act on the baseline R_0 and the stimulation elicited by LPS. However, the rebound is not fully described by the present experimental design. Additional sampling points between 2 and 4 h would improve the picture of rebound.

Although the TNF$_\alpha$ response was not suppressed completely with the highest dose, we still assumed that complete suppression could be produced with higher concentrations of test compound (Eq. (4:5)). The Goodness-of-fit was improved by introducing a series of transit compartments. Multi-phasic TNF$_\alpha$-time courses were observed after test compound intervention. Some of the time TNF$_\alpha$ measurements also picked up the rebound when the doses of test compound were higher. The final model parameters of the rebound- and no-rebound models were determined with reasonable precision (CV < 30%; Table 9).

An IC_{50} of 240 nmol L^{-1} was obtained for the test compound, which corresponds to a steady state exposure that would decrease the TNF_{α}-response following LPS stimulus by 50%. These results are consistent with *ex vivo* (*in vitro*) potency results of test compound using whole blood.

2.5. Case Study 5: challenger identical to PD biomarker, time-course known

2.5.1. Rationale

The oral glucose tolerance test (OGTT) model is widely used in drug assessment for effects on glucose handling and insulin sensitivity/resistance in diabetic conditions. Rodent species are typically used for screening and selecting novel agents that improve glucose handling in diabetic conditions, and PD readouts are insulin and glucose.

2.5.2. Methods

2.5.2.1. Chemicals and reagents. Test compound *Z* used in the study was synthesized in-house at AstraZeneca. All solvents and chemicals used were reagent grade commercially available.

2.5.2.2. Experimental procedure. Forty-two healthy C57BL6/6Jax mice (9–10 weeks old; males, in-house bred, based on founding pairs from the Jax Strater Colony) were housed in groups on a normal light cycle (lights on 6.00 am–6.00 pm) and allowed ad libitum access to standard chow (SDS RM1 diet). Animals were allowed to acclimatize for a minimum of 1 week following arrival to the experimental unit and were randomly assigned to different groups based on their body weight. Mice were fasted for 16 h before glucose administration. A tail-prick blood sample was taken at baseline to allow Accu-chek measurement of glucose before compound administration. Mice were then dosed orally with vehicle (HPMC/Tween) or either 10, 30 or 100 mg/kg of compound Z. At 30 min after the compound dose was given, a glucose load of 2 g kg^{-1} was administered by oral gavage. In conscious mice, tail prick samples for blood glucose measurement (Accu-chek) were then taken at 0, 10, 25, 40, 60, 90 min post glucose load. Blood samples of 5 μL were taken at 0, 40, and 90 min post glucose dose for test compound exposure measurements. At the end of the experiment, all mice were euthanized using rising CO_2 and cervical dislocation, and a terminal cardiac blood sample was obtained for analysis of compound exposure. All animal procedures were approved by the British Home Office Animal Scientific Procedures Act 1986. Fig. 15 shows a schematic representation of the design elements.

2.5.2.3. Bioanalysis of test compound concentration. Blood samples were protein precipitated with ice-cold acetonitrile (Sigma–Aldrich) containing a generic internal standard compound from the AstraZeneca compound library. The samples were then mixed and centrifuged at 4500*g* for 10 min. A sample of the supernatant (50 μL) was removed and diluted with 300 μL of water prior to injection (50 μL) onto the LC–MS/MS system. Samples were analyzed on a TSQ Quantum Vantage mass spectrometer (ThermoFisher Scientific, Hemel Hempstead, UK). Chromatography was performed on a Max-RP (50 mm × 2.1 mm ID, 5 μm) HPLC column (Phenomenex, Macclesfield, UK) with a mobile phase consisting of water containing 0.1% formic acid and methanol containing 0.1% formic acid. After analysis, the results were quantified using QuickCalc™ software (Gubb Inc., Alpharetta, Georgia, USA) by back calculation against the relevant calibration curve. Free test-compound concentrations were calculated based on measured concentrations in blood and corrected using a constant free fraction f_u. Free fraction values were generated in house *in vitro* using previously published methodology.

Table 8
Final kinetic parameter estimates and their precision (CV%).

Parameter	Units	Estimate	CV%
CL	L h^{-1} kg^{-1}	2.2	10
CL_d	L h^{-1} kg^{-1}	0.3	28
V	L kg^{-1}	2.3	17
V_t	L kg^{-1}	4.8	51

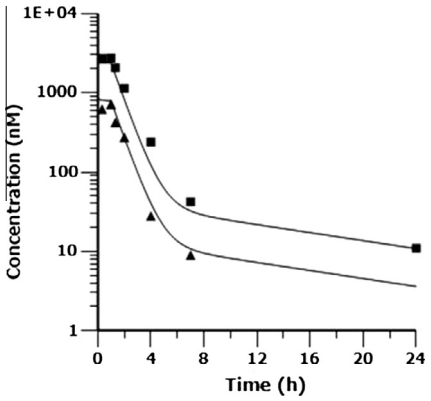

Fig. 13. Semilogarithmic plot of concentration–time data of experimental (symbols) and model predictions (solid lines) of drug levels after i.v. bolus + constant i.v. infusion regimens of test compound at 1 mg kg^{-1} bolus + 1 mg kg^{-1} h^{-1} infusion (solid up-triangles), or 2.9 mg kg^{-1} bolus + 3.1 mg kg^{-1} h^{-1} infusion (solid squares) (n = 4).

2.5.2.4. Pharmacokinetic and pharmacodynamic methods. The average of the measured drug concentrations at each time point (0, 40 and 90 min post glucose) within each group (n = 10 mice per time point and dose level) was calculated. A table function was used to interpolate all test-compound exposure levels between the sampled concentrations. These drug concentrations were then used as covariates in the pharmacodynamic model (Eq. (5:1)).

A turnover model was selected to describe the time course of the glucose biomarker.

$$\frac{dR}{dt} = Input_{OGTT} + k_{in} - k_{out} \cdot (S(C,R) + R) \qquad (5:1)$$

where k_{in}, $S(C, R)$ and k_{out} are the turnover rate, the stimulatory function of test compound and fractional turnover rate, respectively. $Input_{OGTT}$ represents the glucose first-order input function following a 2 g kg^{-1} oral dose of glucose.

$$Input_{OGTT} = \frac{K_a \cdot Dose_{OGTT}}{V} \cdot e^{-K_a \cdot t} \qquad (5:2)$$

where K_a is the glucose absorption rate constant, $Dose_{OGTT}$ is the glucose load (2 g kg^{-1} = 11 mmol kg^{-1}) and V is the volume of distribution of glucose. The stimulatory function of $S(C, R)$ is mathematically described as a logarithmic function of the test compound concentrations but also proportional to the change $(R - R_0)$ from baseline R_0 in blood glucose concentration.

$$S(C,R) = m \cdot \log(1 + C) \cdot (R - R_0) \qquad (5:3)$$

The m parameter is the slope of the log-linear portion of the concentration–response curve.

Eq. (5:4) gives the relationship of the biomarker response R and different levels of test compound intervention on the glucose challenge.

$$R = R_0 \cdot \frac{1}{m \cdot \log(1 + C) \cdot (R - R_0)} \qquad (5:4)$$

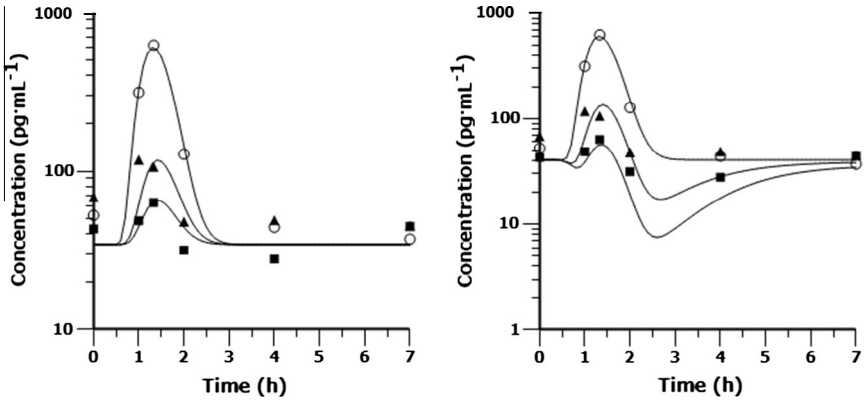

Fig. 14. Left: Semilogarithmic plots of TNF_α concentration–time data of experimental (symbols) and rebound model predictions (solid lines) after an intravenous challenge dose of 1 μg kg^{-1} mL^{-1} in NaCl in cynomolgus monkeys (n = 8 in vehicle group and n = 4 in treatment groups) and different doses of test item at 0 mg kg^{-1} (vehicle; open circles, n = 8), 1 mg kg^{-1} bolus followed by a 1 mg kg^{-1} h^{-1} infusion (solid up triangles), 2.9 mg kg^{-1} bolus followed by a 3.1 mg kg^{-1} h^{-1} infusion (solid squares). Right: Same data fitted with a basic turnover model that does not allow a rebound.

Table 9
Final TNF_α (biomarker) parameter estimates and their relative standard deviation (CV%).

Parameter	Units	Rebound model		Basic turnover	
		Estimate	CV%	Estimate	CV%
k_{out}	pg mL^{-1} h^{-1}	10.7	2	10.0	2
R_0	pg mL^{-1}	40.7	19	34.4	18
k'	h^{-1}	8.4	5	14.8	5
A		390	23	4317	25
IC_{50}	nM	240	18	145	28

2.5.2.5. Numerics. Phoenix WinNonlin 6.3, with a matrix exponent differential equation solver, was used to fit the data. An additive error model was used. Plasma test compound concentration was used as a covariate and all time-courses were simultaneously regressed.

2.5.3. Results and discussion

The oral glucose tolerance test (OGTT) is a commonly used challenge design in early discovery of new experimental compounds for the treatment of type II diabetes. Blood glucose concentrations are frequently monitored for 90 min following an oral dose of glucose. Intervention with a test compound reduces the extent of glucose exposure compared to control animals. In this Case Study, the test compound was shown to reverse blood glucose to normal concentrations in a dose-dependent manner in mice (Fig. 16 and Table 10).

The regressed turnover model was able to simultaneously describe the glucose-time course following different doses of the glucose-lowering test compound in the blood in the OGTT study. Results of the regressions are shown in Fig. 16 and Table 11. Generally, the parameters had good precision. A peak-shift towards the left was seen in glucose biomarker response with increasing doses of test compound since a linear drug-stimulatory function was acting on the loss of response.

The action of the test compound is assumed to be proportional to the blood glucose levels above baseline and not to the absolute blood glucose concentration *per se*. The intended mechanism of the compound's action is compatible with a lack of hypoglycemia, and indeed hypoglycemia has not yet been observed with this compound in this or other experiments.

3. Discussion

We have described and summarized *in vivo* PK/PD modeling in 5 Case Studies that used drug challenge designs across therapeutic areas, each with varying characteristics. These Case Studies thus differ with respect to information content, and suggestions are given how quantitative PK/PD modeling may be rationally approached in a particular situation. Pivotal findings in each of the Case Studies are discussed below and summarized in Table 12, including recommendations about the corresponding design elements.

3.1. Case Study 1 – Sephadex-induced eosinophilia

The Sephadex challenge treatment was clearly effective at triggering the PD response, at a level well above the (minor) stress/handling-induced changes in the control (vehicle) group (Fig. 3). Thus, whereas the inter-individual variability in eosinophil numbers is large, the separation between Sephadex- (Eq. (1:1)) and vehicle- (Eq. (1:2)) treated groups was nonetheless demonstrated (Table 2). The question may still arise whether the large variation in eosinophil response is due to variable Sephadex time-courses across different animals. The two-parameter Sephadex function (Eq. (1:1)) had acceptable parameter precision in A_1 and K_{p1}. However, possibly two or more Sephadex doses combined with full challenger- and biomarker-time courses would further improve the robustness of these estimates. In addition, if eosinophil time courses after test compound intervention can be appended to the

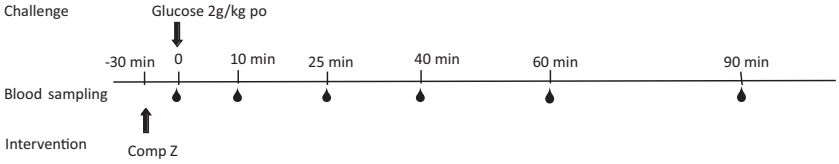

Fig. 15. Schematic representation of the design of Case Study 5. A range of test-compound doses or vehicle (HPMC/Tween control) were injected 30 min before administration of the glucose challenge (n = 10–12 animals per group).

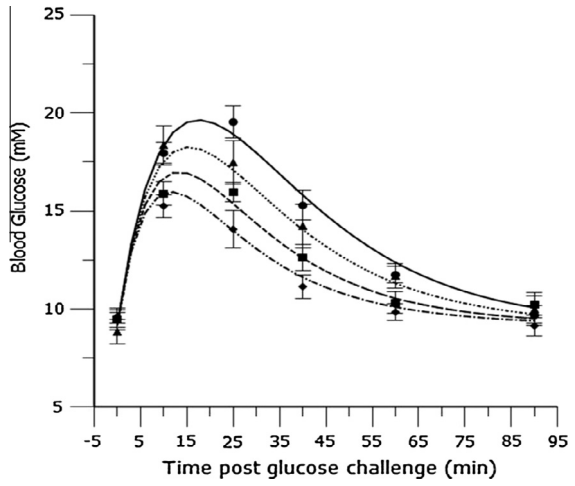

Fig. 16. Mean blood glucose and model prediction in mice OGTT after a single oral dose of either vehicle control (circles) or test compound treatment at 10 (triangles), 30 (squares) or 100 (diamonds) mg kg^{-1}, administered 30 min before a 2 g kg^{-1} oral dose of glucose challenge (n = 10–12 mice per group; data shown are means ± SEM).

regression, the parameter precision will increase further and allow separation of test compound (IC_{50}) and system (k_{out}) parameters. The same total number of animals (Fig. 3) can then be better quantitatively utilized if each animal is given its individual dose and the samples are then spread out in time (to cover the return back to baseline); the data can then be modeled.

3.2. Case Study 2 – antagonism of $IL_{1\beta}$-induced IL_6 elevation

Case Study 2 showed that the time course of cytokine response (IL_6) induced by $IL_{1\beta}$ challenge was suppressed by pretreatment intervention using Anakinra. The compound also reversed the $IL_{1\beta}$ induced cytokine IL_6 elevation in the mouse in a dose-dependent manner.

This Case Study is the most complete design of the five examples discussed. It contained time courses of test compound (drug) and challenger ($IL_{1\beta}$), as well as cytokine response (IL_6). The results from this set-up updated with higher resolution data on IL_6 response to new IL_1 antagonists, combined with a mixed-effects modeling approach, can be expected to provide a good platform for optimization and selection of novel IL_1 receptor antagonist candidates. The turnover properties (system) and challenge profile (system) were separated from the test compound properties (potency, etc.), hence allowing a better translation of preclinical data from different experiments and compounds to humans.

3.3. Case Study 3 – reversal of collagen-induced arthritis (CIA)

For Case Study 3, we developed a mathematical model of the CIA progression. In the absence of information of the challenger (Freund's adjuvant) time-course dynamics, swelling scores over time, with and without the intervention of the test compound, were used to describe arthritis progression. A one-compartment model that served as a smoothing function and input to the inhibitory drug mechanism function of the PD biomarker model described the exposure profiles of the test compound after oral dosing.

The response and progression of the PD biomarker paw-swelling was described by a modified version of a previously published turnover model (inhibition of production) for paw edema in arthritic rats (Lon et al., 2011). The inflammatory process is very dynamic and changes in the inflammatory stages may vary from day to day; thus, it is difficult to follow the precise disease development in the joints of each study animal. To capture the overall delay of onset of the PD biomarker response, we combined the turnover model with a series of four transit compartments. Others have incorporated up to 19 transduction steps to account for the time delay of paw swelling and five additional transduction steps to account for the time delay of natural remission (Liu et al., 2013). Our data, however, suggest that a 4-step transit model would suffice. The natural remission of CIA, which has been observed in animal models (Luross and Williams, 2001), was captured by the parameter R_{deg}. This parameter represents a first-order decline ($t_{1/2} \sim 30$ days) of the turnover rate k_{in} (Earp et al., 2008a, 2008b; Lon et al., 2011), suggesting that an extended observational period may be needed. The bi-phasic decline in the paw-swelling suggests other model structures, including removal of the time-dependent attenuation of certain parameters. The turnover rate was mathematically described as a function of time that was dependent on the degree of swelling. The time-dependent change in either the synthesis or elimination rates was introduced by Post et al. (2005). It is therefore possible that a more mechanistically based approach to model these data that also captures multiple challenges over time may help further refining modeling in this setting.

Exposure (test compound or vehicle control) and biomarker (swelling score) data were obtained simultaneously from all animals. Although the model generated acceptable predictions for swelling-score time profiles and reasonable parameter estimates, the IC_{50} may be biased because exposure concentration data were available only after a single challenge dose.

From a PD point-of-view, it should be noted that the response readout in this Case is based on an arbitrary summed scoring scale with a maximum possible number of 12. This in turn implies that a drug-induced reduction of the PD response from, say, 10 to 5, does not necessarily mean that the CIA process is inhibited by 50% at the actual target level, only that the qualitatively scored readout is

Table 11
Final model parameters and their precision (CV%).

Parameter	Units	Estimate	CV%
K_a	min^{-1}	0.053	17
V	kg^{-1}	0.36	20
R_0	mM	9.2	2
k_{out}	min^{-1}	0.062	18
m	μM^{-1}	0.48	13

Table 10
Mean compound concentration in mouse OGTT after a single oral dose of either vehicle (control), or test compound given at 10, 30 or 100 mg kg^{-1}, administered 30 min before a 2 g kg^{-1} oral challenge dose of glucose (N = 10 mice per group, SEM = standard error of the mean).

Time, post glucose load (min)	Test compound concentration in blood (μM)					
	10 mg kg^{-1}		30 mg kg^{-1}		100 mg kg^{-1}	
	Mean	SEM	Mean	SEM	Mean	SEM
0	0.949	0.106	3.172	0.235	8.377	0.789
40	0.810	0.100	3.032	0.205	9.353	0.394
90	0.535	0.093	2.131	0.221	6.813	0.520

Table 12
Summary of major findings and suggested improvements for future designs.

Case Study	Points to consider	Major findings	Suggested improvements of design elements
1	Baseline response	• Needs to reduce PD response variability	• Complete time course of PD response
	Time delay	• Information about challenger may explain some PD response variability	• Time-series of test compound and challenger at $\geqslant$2 dose levels to validate PD response variability and improve the precision of model parameters
		• Expected shift in peak-time with intervention of test compound	
2	Baseline response	• Includes challenger, test compound, and PD response time courses	• Improved resolution of PD response at C_{max} & t_{max}
	Time delay (peak-shift)	• High parameter precision	• Expected shift in peak-time with intervention of test compound
	Transduction steps	• Expected shift in peak-time with intervention of test compound	
3	Baseline response	• PD response followed towards return to baseline which means improved predictions	• Include challenger time-course
	Time delay (peak-shift)	• High parameter precision	• Run $\geqslant$1 dose of challenger
	Transduction steps	• Expected shift in peak-time with intervention of test compound	
4	No baseline response	• Extended sampling of PD response	• Include challenger time-course
	Time delay (peak-shift)	• Reasonable parameter precision	• Improve sampling at rebound
	Transduction steps	• Expected shift in peak-time with intervention of test compound	• Run $\geqslant$1 dose of challenger
	Slope differences		
	Rebound		
5	Baseline response	• OGTT model; challenger = PD response marker	• Run $\geqslant$1 glucose challenge dose
	Time delay	• Reasonable parameter precision	
	Peak-shift	• Observed shift in peak-time with intervention of test compound	

halved. Infrared thermography (to monitor changes in skin temperature) has been proposed as a refinement of the model, potentially conferring a more sensitive and objective method to assess degree of inflammation and effects of putative therapeutic agents (Jasemian et al., 2011).

However, the turnover model captured the current PD biomarker data reasonably. It could therefore serve as a basis for future studies where the inclusion of biomarkers would give additional insights and allow a more quantitative assessment of disease-modifying drugs in the rat CIA model (Earp et al., 2008a, 2008b, 2009).

3.4. Case Study 4 – prevention of LPS-induced increases in TNF_α

Acute cytokine release models provide an example of challenge tests where the stimulus elicits a rapid but transient kinetic of a biomarker response (Wollenberg et al., 1993). These types of models in rodents are often used as initial *in vivo* PD models for immune-modulating agents in drug discovery (Beck et al., 2002; Zhang et al., 2004).

In Case Study 4, cynomolgus monkeys were challenged by intravenous LPS administration and changes in the pro-inflammatory cytokine TNF_α were studied in the presence or absence of prophylactic infusion of an inhibitory test compound. No data on the LPS challenger kinetics were available (Remick, 1995; Malerich and Elston, 2006). The turnover data of TNF_α biomarker response after LPS challenge in the vehicle-treated animals was described using a model with a time-dependent stimulatory function acting on the turnover rate k_{in}. A number of transit compartments were incorporated to adequately capture the rapid changes in TNF_α kinetics after a delayed onset of action. Acute cytokine release has previously been modeled with discontinuous functions, allowing the induced formation of TNF_α to take place only for a defined period (Gozzi et al., 1999; Chakraborty et al., 2005; Wyska, 2010). In our example, we propose a continuous model using a stimulatory function coupled to transit compartments.

Physiologically, there is no observable baseline concentration of TNF_α in blood. The cytokine is only released into blood from activated monocytes in response to an immunological stimulus (Malerich and Elston, 2006). In this Case Study, already at t_0, TNF_α was quantifiable in the systemic circulation of the test animal and levels returned to the initial values at 24 h post stimulus, which is incorporated into the suggested model, and R_0 reflects a baseline concentration of about 40 pg mL^{-1}.

The drug-induced inhibition acts on the LPS stimulatory function S(LPS). Hence, predicted TNF_α levels do not decrease below R_0. The IC_{50} value describes the steady-state concentration of the test item that would lead to a 50% reduction in the TNF_α response following LPS challenge.

3.5. Case Study 5 – drug-induced effects on glucose handling (OGTT model)

OGTT is a commonly used test carried out in mice; it is considered the most physiological test, since it mimics the normal route of administration of dietary glucose in man (Pacini et al., 2013). Data generated using this model have been analyzed in several different ways to obtain information regarding insulin sensitivity, but analyses commonly focus on the area under the glucose concentration–time curves (Pacini et al., 2005).

Glucose and insulin dynamics have previously been analyzed using turnover models after simultaneous administration of compounds that alter glucose homeostasis in rodents (Lima et al., 2004; Gao and Jusko, 2012; Jin and Jusko, 2009). However, in these situations, no exogenous glucose challenge has been given. Therefore, those models cannot be directly applied to OGTT data where the baseline changes as a result of the challenge.

In humans, an integrated glucose-insulin model has been used to describe OGTT data (Jauslin et al., 2007; Silber et al., 2010). We took glucose absorption into account using either a transit compartment model or an empirical model with a series of zero order inputs. Additionally, we propose a multi-compartment model for glucose distribution in the body coupled to a more complex control mechanism of glucose-insulin.

In Case Study 5, the glucose absorption was assumed to follow a 1st order process. We proposed a simplified acute turnover model in which the expected effect of insulin on blood glucose control is described as clearance of blood glucose concentrations above baseline. This was done in light of no available insulin data (due to blood volumes) and only limited data for glucose measurements. Despite these limitations, the acute effect model successfully described the magnitude and duration of the blood glucose turnover after administration of vehicle control and test compound in an OGTT setting.

Table 13
Comparisons of models.

Case Study	Action	Pharmacodynamic relationship	PD behavior
1	Stimulation of k_{in}	$R = R_0 \cdot (1 + S(\text{Sephadex}) + S(\text{Stress}))$	Linear as long as drug action is linear
2	Nonlinear stimulation of k_{in}	$R = R_0 \cdot (1 + P \cdot (C_{IL_{1\beta}} - C_{IL_{1\beta}}(\text{baseline})) \cdot (1 - \frac{C_i}{IC_{50,i}+C_i}))$	Nonlinear drug mechanism function
3	Nonlinear stimulation of k_{in}	$R = R_0(t) \cdot (1 - \frac{I_{max} \cdot C_i^n}{IC_{50}^n + C_i^n})$	Nonlinear drug mechanism function
4	Nonlinear stimulation of k_{in}	$R = R_0 \cdot S(t) = R_0 \cdot (1 + A \cdot k' \cdot t \cdot e^{(-k' \cdot t)} \cdot (1 - \frac{C_i}{IC_{50}+C_i}))$ $R = R_0 \cdot S(t) = R_0 \cdot (1 + A \cdot k' \cdot t \cdot e^{(-k' \cdot t)}) \cdot (1 - \frac{C_i}{IC_{50}+C_i})$	Nonlinear drug mechanism function
5	Log-linear stimulation of k_{out}	$R = R_0 \cdot \frac{1}{m \cdot \log(1+C) \cdot (R-R_0)}$	Nonlinear since drug acts on k_{out}

The inhibitory 'drug-mechanism function' on blood glucose was assumed to follow a log relationship rather than a more complicated but biologically mechanistic model, due to the observational range of concentration–response data. This obviously limits the ability of this model to predict effects beyond the test compound exposures and blood glucose concentrations used in the Study. Another improvement would be to describe the plasma test compound concentrations with a mathematical function, rather than as a table function in the analysis. This would facilitate the ability to use the proposed model to predict effects at alternative dosing schedules.

The models in the Case Studies are compared and described mathematically in Table 13. All of them suggest a peak-shift to the left in PD biomarker response with increasing doses of test compound. This is due to the nonlinear drug mechanism functions (Case Studies 2–4) or the log-linear stimulatory function on k_{out} (Case Study 5).

4. General remarks and considerations

As evident by our model assessments, optimal study design requires premeditated integration of several elements to fit modeling input requirements. Thus, while the basics of choosing and characterizing the actual model best suited for screening and translatable predictions (*e.g.*, PD 'disease' biomarker validation across species) are obviously crucial in any context, careful attention should also be paid to relevant (drug and challenger) PK and PD aspects, and what might influence these in the particular model selected (Gabrielsson and Green, 2009; Gabrielsson et al., 2009; Gabrielsson and Weiner, 2010; Gabrielsson and Hjorth, 2012). For example, pathophysiological alterations in a particular disease model may influence PK (*e.g.*, absorption, distribution, elimination, etc.) as well as PD response (*e.g.*, target sensitivity, transduction and/or downstream processes, compensatory adjustments, etc.) variables, thereby affecting the corresponding parameter readout and modeling approach (*cf.*, *e.g.*, Case Studies 3 and 4). As long as the dynamics of such a process are under reasonable control the aforementioned complexities should not present a problem, but serves to illustrate the general principle of working with adequately controlled, robust models to optimize PK/PD modeling and subsequent predictions for new candidate drugs. It also follows that not only should the PD response time-course be monitored and defined in the disease model under study, but also PK and challenger time-courses should be run under identical conditions.

Furthermore, the PD response readout may be more or less distant from the actual target intended for drug intervention, with one or several steps in between the primary action and the actual PD response biomarker display. This, however, does not preclude usefulness of data even from *in vivo* scoring models (*cf.* Case Study 3) or other comparable situations (*e.g.*, body weight, motor activity, specific behavioral alterations), when modeling the PK/PD relation – like in Case Study 3. Similarly, in all of the Cases described, the time courses also reflect challenger and drug levels taken at a distance from the actual biomatrix of target and/or therapeutic interest. Thus, while systemic plasma and blood levels are clearly the most easily accessible substitute compartments and clearly useful to the predictions in our Case Studies, it may well be that a more precise PK/PD understanding could have been gained based on knowledge and modeling of the levels in targeted cells, tissues or specific vascular beds (*e.g.*, lung, subcutaneous tissue, liver).

Finally, although not specifically presented with data in the current set of Case Studies, there are obviously multiple examples of challenge test situations for different models of CNS dysfunction and allied processes. In these instances, the PD biomarker output may be neurochemical, electrophysiological, autonomic, neuroendocrine, molecular imaging, or – more often – typically a

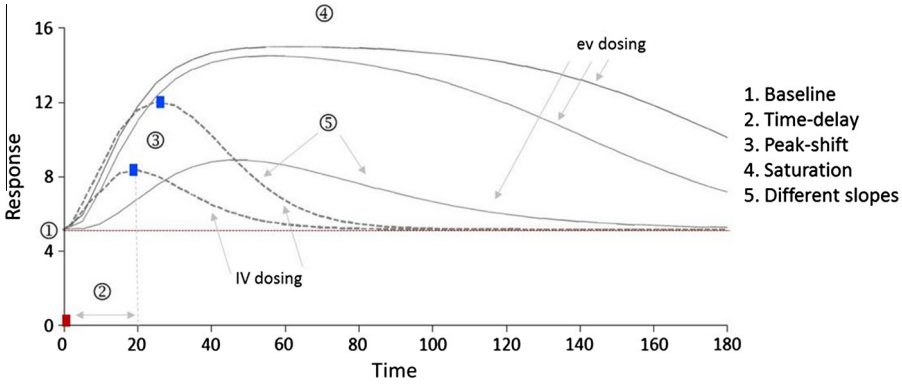

Fig. 17. Schematic presentation of the pivotal characteristics of PD data. Data contain a baseline ①, time-delay between peak exposure ② (not measured) and peak of response, peak-shift with increasing doses ③, saturation at the highest dose ④ and different slopes of decline post-peak, depending on route of administration ⑤. Since response-time data were available after both intravenous (dashed lines) and subcutaneous (solid lines) dosing, the biophase availability could be estimated as a model parameter. See also Peletier et al., 2005; Gabrielsson and Peletier (2013).

behavioral readout, to mention a few. Examples include models to screen for novel agents for putative antipsychotic action (*e.g.*, reversal of D-amphetamine single neuron and motor effects; Haracz et al., 1993), for reversal of cognitive dysfunction (*e.g.*, scopolamine-induced memory impairment; Buccafusco, 2009), for assessing analgetic drug effects (*e.g.*, thermic, mechanical, inflammatory, etc., pain models; Berge, 2011), pro/anti-convulsive properties (*e.g.*, pentylenetetrazole-induced seizures; Löscher, 2009) for optimization of treatment protocols and/or exploration of specific disease processes (*e.g.*, imaging methods like PET; Lee and Farde, 2006), and in connection with various types of physiological states (*e.g.*, diet- or stress-induced changes in food intake or anxiety-like behavior, respectively; Ravinet Trillou et al., 2003; Jaggi et al., 2011). While outside the scope of our report, for a broader discussion on animal models of CNS disease/dysfunction in general, including limitations and suggestions for the future, we refer the interested reader to Markou et al. (2009). From the PK/PD modeling point-of-view, however, a similar reasoning and rationale could be applied compared to our Case Studies.

5. Conclusions

In presenting our five Case Studies, we sought to exemplify various experimental designs and how they can be improved to better guide compound selection. Thus, our goal was not to present an in-depth analysis of a specific mathematical model. For this, we refer the reader to the original references. Instead, we intended to illustrate to readers the range of conditions an investigator may encounter in a typical population of normal or diseased animals, and necessary points to consider in experimental design. For instance, in our experience, it is much more informative to obtain a full PD biomarker response-time profile at two or more doses of a particular compound, rather than stacking up cohorts of animals at single time points. We thus argue that the design, analysis and communication of challenge experiments needs a totally different mind-set than has been the case in hypothesis-test driven traditional designs. A quantitative approach similar to the one we advocate for pre-clinical studies has been elegantly advanced by Sheiner (1991) from a drug developmental point of view.

To enhance predictive power, a modeler has to elaborate on the pattern of onset, intensity and duration of PD response. We have discussed some principal aspects of modeling PD readout data, such as the influence of baseline (1 in Fig. 17), time-delays (2), transduction (3), peak-shifts (4) and saturation or lack of saturation (5). These features are schematically illustrated in Fig. 17 below. We also highlighted the importance of actually measuring the challenger (*e.g.*, $IL_{1\beta}$ in Case Study 2) rather than making indirect inferences about its behavior by deconvoluting the PD biomarker response. For further information about the latter approach on mixture data analyses see Gabrielsson and Peletier (2013).

If no prior information is available about the PD mechanism of action, model building may start with a few points of insight on the proposed PD response biomarker, such as baseline behavior, time-delays, peak-shifts with increasing doses, saturation of response at higher doses and decline towards baseline (*cf.*, Fig. 17). For optimal outcome, however, study data should include monitoring of directly target-related and translatable biomarkers across several species, concomitant with measurements of plasma drug concentrations across time- and dose ranges, plasma protein binding of the drug *ex vivo* (or, if not possible, *in vitro*), and knowledge of the presence and activity of potential active metabolites that may influence the results (Gabrielsson and Peletier, 2013; Gabrielsson et al., 2014).

Typically, time-series analyses of challenger- and biomarker-time data are necessary when an accurate and precise estimate of the test compound pharmacodynamic properties is desired. Erosion of data or the single-point assessment of drug action after a challenge test should generally be avoided, particularly in situations where one expects time-curve shifts, tolerance/rebound, impact of disease or hormetic (Calabrese, 2013) concentration–response relationships to occur.

Disclosure statement

JG is an employee of the Swedish Agricultural University. LAP is Professor Emeritus in the Dept. of Mathematics at Leiden University. SHj, RP, PM and PD are or were employees of AstraZeneca. BV and SH are employees of Novartis Institutes for Biomedical Research. The proposed thoughts are our own and not necessarily sanctioned by our respective organizations.

Acknowledgements

We gratefully acknowledge the support and scientific contributions from colleagues at AstraZeneca R&D Mölndal (Sweden) and at Novartis Institutes for BioMedical Research, Basel (Switzerland).

References

Beck, G., Bottomley, G., et al., 2002. (E)-2(R)-[1(S)-(hydroxycarbamoyl)-4-phenyl-3-butenyl]-2′-isobutyl-(methanesulfonyl)-4-methylvalerohydrazide (Ro 32-7315), a selective and orally active inhibitor of tumor necrosis factor-α convertase. J. Pharmacol. Exp. Ther. 302, 390–396.

Beevart, L., Vervoordeldonk, M.J., Tak, P.P., 2010. Evaluation of therapeutic targets in animal models of arthritis: how does it relate to rheumatoid arthritis? Arthritis Rheum. 62, 2192–2205.

Berge, O.-G., 2011. Predictive validity of behavioural animal models for chronic pain. Br. J. Pharmacol. 164, 1195–1206.

Bondesson, J., 1997. The mechanisms of action of disease-modifying antirheumatic drugs: a review with emphasis on macrophage signal transduction and the induction of proinflammatory cytokines. Gen. Pharmacol. 29, 127–150.

Brooks, P.M., 2006. Rheumatoid arthritis: aetiology and clinical features. Medicine 34, 379–382.

Buccafusco, J.J., 2009. The revival of scopolamine reversal for the assessment of cognition-enhancing drugs. In: Buccafusco, J.J. (Ed.), Frontiers in Neuroscience Series; Methods of Behavior Analysis in Neuroscience, second ed. CRC Press, Boca Raton, FL (Chapter 17).

Bueters, T.J.H., Hoogstraate, J., Visser, S.A.G., 2009. Correct assessment of new compounds using in vivo screening models can reduce false positives. Drug Discov. Today 14, 89–94.

Calabrese, E., 2013. Hormetic mechanisms. Crit. Rev. Toxicol. 43, 580–606.

Chakraborty, A., Yeung, S., Pyszczynski, N.A., Jusko, W.J., 2005. Pharmacodynamic interactions between recombinant mouse interleukin-10 and prednisolone using a mouse endotoxemia model. J. Pharm. Sci. 94, 590–603.

Earp, J.C., DuBois, D.C., Molano, D.S., Pyszczynski, N.A., Keller, C.E., Almon, R.R., Jusko, W.J., 2008a. Modeling corticosteroid effects in a rat model of rheumatoid arthritis I: mechanistic disease progression model for the time course of collagen-induced arthritis Lewis rats. J. Pharmacol. Exp. Ther. 326, 532–545.

Earp, J.C., DuBois, D.C., Molano, D.S., Pyszczynski, N.A., Keller, C.E., Almon, R.R., Jusko, W.J., 2008b. Modeling corticosteroid effects in a rat model of rheumatoid arthritis II: mechanistic pharmacodynamic model for dexamethasone effects in Lewis rats with collagen-induced arthritis. J. Pharmacol. Exp. Ther. 326 (2), 546–554.

Earp, J.C., DuBois, D.C., Almon, R.A., Jusko, W.J., 2009. Quantitative dynamic models of arthritis progression in the rat. Pharm. Res. 26, 196–203.

Eder, C., 2009. Mechanisms of interleukin-1 beta release. Immunobiology 214, 543–553.

Evaldsson, C., Ryden, I., Uppugunduri, S., 2011. Isomaltitol exacerbates neutrophilia but reduces eosinophilia: new insights into the Sephadex model of lung inflammation. Int. Arch. Allergy Immunol. 154, 286–294.

Fredericks, Z.L., Forte, C., Capuuano, V., Zhou, H., Vanden Bos, T., Carter, P., 2004. Identification of potent human anti-IL−1R1 antagonistic antibodies. Protein Eng. Des. Sel. 17, 95–106.

Gabrielsson, J., Green, R., 2009. Quantitative pharmacology or pharmacokinetic pharmacodynamic integration should be a vital component in integrative pharmacology. J. Pharmacol. Exp. Ther. 331, 767–774.

Gabrielsson, J., Hjorth, S., 2012. Quantitative Pharmacology: An Introduction to Integrative Pharmacokinetic-Pharmacodynamic Analysis, first ed. Swedish Pharmaceutical Press, ISBN 9 789197 945233.

Gabrielsson, J., Peletier, L.A., 2013. Mixture dynamics: dual action of inhibition and stimulation. Eur. J. Pharm. Sci. 50, 215–226.

Gabrielsson, J., Weiner, D., 2010. Pharmacokinetic-Pharmacodynamic Data Analysis: Concepts and Applications, fourth ed. Swedish Pharmaceutical Press, ISBN 13 978 91 9765 100 4 (2nd print).

Gabrielsson, J., Dolgos, H., Gillberg, P.-G., Bredberg, U., Benthem, B., Duker, G., 2009. Early integration of pharmacokinetic and dynamic reasoning is essential for optimal development of lead compounds: strategic considerations. Drug Discov. Today 14, 358–372.

Gao, W., Jusko, W.J., 2012. Modeling disease progression and rosiglitazone intervention in type 2 diabetic Goto-Kakizaki rats. J. Pharmacol. Exp. Ther. 341, 617–625.

Gozzi, P., Påhlman, I., Palmér, L., Grönberg, A., Persson, S., 1999. Pharmacokinetic-pharmacodynamic modeling of the immunomodulating agent susalimod and experimentally induced tumor necrosis factor-α levels in the mouse. J. Pharmacol. Exp. Ther. 291, 199–203.

Haddad, E., Underwood, S., Dabrowski, D., Birrell, M., McCluskie, K., Battram, C., Pecoraro, M., Foster, M., Belvisi, M., 2002. Critical role for T cells in Sephadex-induced airway inflammation: pharmacological and immunological characterization and molecular biomarker identification. J. Immunol. 168, 3004–3016.

Haracz, J.L., Tschanz, J.T., Wang, Z., White, I.M., Rebec, G.V., 1993. Striatal single-unit responses to amphetamine and neuroleptics in freely moving rats. Neurosci. Biobehav. Rev. 17, 1–12.

Hegen, M., Keith Jr, J.C., Collins, M., Nickerson-Nutter, C.L., 2008. Utility of animal models for identification of potential therapeutics for rheumatoid arthritis. Ann. Rheum. Dis. 67, 1505–1515.

Homayoun, H., Khavandgar, S., Namiranian, K., Gaskari, S.A., Dehpour, A.R., 2002. The role of nitric oxide in anticonvulsant and proconvulsant effects of morphine in mice. Epil. Res. 48, 33–41.

Jaggi, A.S., Bhatia, N., Kumar, N., Singh, N., Anand, P., Dhawan, R., 2011. A review on animal models for screening potential anti-stress agents. Neurol. Sci. 32, 993–1005.

Jasemian, Y., Svendsen, P., Deleuran, B., Dagnaes-Hansen, F., 2011. Refinement of the collagen-induced arthritis model in rats by infrared thermography. Br. J. Med. Med. Res. 1, 469–477.

Jauslin, P.M., Silber, H.E., Frey, N., 2007. An integrated glucose-insulin model to describe oral glucose tolerance test data in type 2 diabetics. J. Clin. Pharmacol. 47, 1244–1255.

Jin, J.Y., Jusko, W.J., 2009. Pharmacodynamics of glucose regulation by methylprednisolone. I. Adrenalectomized rats. Biopharm. Drug Dispos. 30, 21–34.

Källstrom, L., Brattsund, R., Lövgren, U., Svensjö, E., Roempke, K., 1985. A rat model for testing anti-inflammatory action in lung and the effect of glucocorticosteroids (GCS) in this model. Agents Actions 17, 355–357.

Lee, C.M., Farde, L., 2006. Using positron emission tomography to facilitate CNS drug development. Trends Pharmacol. Sci. 27, 310–316.

Lima, J.J., Matsushima, N., Kissoon, N., Wang, J., Sylvester, J.E., Jusko, W.J., 2004. Modeling the metabolic effects of terbutaline in β_2-adrenergic receptor diplotypes. Clin. Pharmacol. Ther. 76, 27–37.

Liu, D.Y., Lon, H.K., Wang, L.Y., Dubois, D.C., Almon, R.R., Jusko, W.J., 2013. Pharmacokinetics, pharmacodynamics and toxicities of methotrexate in healthy and collagen-induced arthritic rats. Biopharm. Drug Dispos. 34, 203–214.

Lon, H.K., Liu, D., Zhang, Q., Dubois, D.C., Almon, R.R., Jusko, W.J., 2011. Pharmacokinetic-pharmacodynamic disease progression model for effect of etanercept in Lewis rats with collagen-induced arthritis. Pharm. Res. 28, 1622–1630.

Lon, H.K., Liu, D., Jusko, W.J., 2012. Pharmacokinetic-pharmacodynamic modeling in inflammation. Crit. Rev. Biomed. Eng. 40, 295–312.

Lon, H.K., Liu, D., Dubois, D.C., Almon, R.R., Jusko, W.J., 2013. Modeling pharmacokinetics/pharmacodynamics of abatacept in collagen-induced arthritic rats: a population approach. J. Pharmacokin. Pharmacodyn. 40, 701–712.

Löscher, W., 2009. Preclinical assessment of proconvulsant drug activity and its relevance for predicting adverse events in humans. Eur. J. Pharmacol. 610, 1–11.

Luross, J.A., Williams, N.A., 2001. The genetic and immunopathological processes underlying collagen-induced arthritis. Immunology 103, 407–416.

Malerich, P., Elston, D.M., 2006. Introduction to TNF/pathophysiology of TNF. In: Weinberg, J.M., Buchholz, R. (Eds.), TNF-alpha Inhibitors. Birkhäuser Verlag, Basel, ISBN: 978 3 7643 7248 4 (print) 978 3 7643 7438 9 (online).

Markou, A., Chiamulera, C., Geyer, M.A., Tricklebank, M., Steckler, T., 2009. Removing obstacles in neuroscience drug discovery: the future path for animal models. Neuropsychopharmacology 34, 74–89.

Mitchell, L.A., Channell, M.M., Royer, C.M., Ryter, S.W., Choi, A.M.K., McDonald, J.D., 2010. Evaluation of inhaled carbon monoxide as an anti-inflammatory therapy in a nonhuman primate model of lung inflammation. Am. J. Physiol. Lung Cell. Mol. Physiol. 299, L891–L897.

Nolan, R.P., Bree, A.G., Zutshi, A., 2013. A mechanistic pharmacodynamic model of IRAK-4 drug inhibition in the Toll-like receptor pathway. J. Pharmacokin. Pharmacodyn. 40, 609–622.

Pacini, M.G., Brazzale, A.R., Ahren, B., 2005. Comparative evaluation of simple insulin sensitivity methods based on the oral glucose tolerance test. Diabetologia 48, 748–751.

Pacini, M.G., Omar, B., Ahren, B., 2013. Methods and models for metabolic assessment in mice. J. Diabetes Res.. Article ID 986906.

Peletier, L.A., Gabrielsson, J., den Haag, J., 2005. A dynamical systems analysis of the indirect response model with special emphasis on time to peak response. J. Pharmacokin. Pharmacodyn. 32, 607–654.

Post, T.M., Freijer, J.I., DeJongh, J., Danhof, M., 2005. Disease system analysis: basic disease progression models in degenerative disease. Pharm. Res. 22, 1038–1049.

Ravinet Trillou, C., Arnone, M., Delgorge, C., Gonalons, N., Keane, P., Maffrand, J.P., Soubrie, P., 2003. Anti-obesity effect of SR141716, a CB1 receptor antagonist, in diet-induced obese mice. Am. J. Physiol. Regul. Integr. Comp. Physiol. 284, R345–R353.

Remick, D.G., 1995. Applied molecular biology of sepsis. J. Crit. Care 10, 198–212.

Sheiner, L., 1991. The intellectual health of clinical drug evaluation. Clin. Pharmacol. Ther. 50, 4–9.

Silber, H.E., Frey, N., Karlsson, M.O., 2010. An integrated glucose-insulin model to describe oral glucose tolerance test data in healthy volunteers. J. Clin. Pharmacol. 50, 246–256.

Wang, Q., Zhang, Y., Hall, J.P., Lin, L.L., Raut, U., Mollova, N., Green, N., Cuozzo, J., Chesley, S., Xu, X., Levin, J.I., Patel, V.S., 2007. A rat pharmacokinetic/pharmacodynamic model for assessment of lipopolysaccharide-induced tumor necrosis factor-alpha production. J. Pharmacol. Toxicol. Meth. 56, 67–71.

Wollenberg, G.K., DeForge, L.E., Bolgos, G., Remick, D.G., 1993. Differential expression of tumor necrosis factor and interleukin-6 by peritoneal macrophages in vivo and in culture. Am. J. Pathol. 143, 1121–1130.

Wyska, E., 2010. Pharmacokinetic-pharmacodynamic modeling of methylxanthine derivatives in mice challenged with high-dose lipopolysaccharide. Pharmacology 85, 264–271.

Zhang, Y., Hegen, M., Xu, J., Keith Jr, J.C., Jin, G., Du, X., Cummons, T., Sheppard, B.J., Sun, L., Zhu, Y., Rao, V.R., Wang, Q., Xu, W., Cowling, R., Nickerson-Nutter, C.L., Gibbons, J., Skotnicki, J., Lin, L.L., Levin, J., 2004. Characterization of (2R,3S)-2-({[4-(2-butynyloxy) phenyl]sulfonyl} amino)-N,3-dihyroxybutanamide, a potent and selective inhibitor of TNF-α converting enzyme. Int. Immunopharmacol. 4, 1845–1857.